A Stochastic Single-Molecule Event Triggers Phenotype Switching of a Bacterial Cell

A stochastic single-molecule event triggers phenotype switching of a bacterial cell

Paul J. Choi,[1]* Long Cai,[1,‡]* Kirsten Frieda,[1,§] X. Sunney Xie[1†]

[1]Department of Chemistry and Chemical Biology, Harvard University, Cambridge, MA 02138

* These authors contributed equally to this work.

[†] To whom correspondence should be addressed. E-mail: xie@chemistry.harvard.edu

[‡] Present address: Division of Biology, California Institute of Technology, Pasadena, CA 91125

[§] Present address: Biophysics Program, Stanford University, Stanford, CA 94305

ABSTRACT

We investigate the molecular mechanism of how an *E. coli* cell with the *lac* operon switches from one phenotype to another by monitoring fluorescently labeled lactose permease with single-molecule sensitivity. At intermediate inducer concentrations, a population of genetically identical cells exhibits two phenotypes: induced cells with highly fluorescent membranes and uninduced cells with a small number of membrane-bound permeases. We find that this basal level expression results from partial dissociation of the tetrameric lactose repressor from one of its operators on looped DNA. In contrast, infrequent events of complete dissociation of the repressor from DNA result in large bursts of permease expression that trigger induction of the *lac* operon. Hence, a stochastic, single molecular event determines a cell's phenotype.

Genetically identical cells in the same environment can exhibit different phenotypes, and a single cell can switch between distinct phenotypes in a stochastic manner (*1-4*). In the classic example of lactose metabolism in *E. coli,* the *lac* genes are fully expressed for every cell in a population under high extracellular concentrations of inducers, such as the lactose analog methyl-β-D-thiogalactoside (TMG). However, at moderate inducer concentrations, the *lac* genes are highly expressed in only a fraction of a population, which may confer a fitness advantage for the entire population (*5*). Here we study the

molecular mechanism that controls the stochastic phenotype switching of a single cell.

Lactose metabolism is controlled by the *lac* operon (*6*, *7*), which consists of the *lacZ*, *lacY*, and *lacA* genes encoding beta-galactosidase, lactose permease, and transacetylase, respectively. Expression of the operon is regulated by a transcription factor, the *lac* repressor (*8*), which dissociates from its specific binding sequences of DNA, the *lac* operators, in the presence of inducer to allow transcription (Fig. 1A). The production of the permease increases inducer influx (*9*), resulting in positive feedback on permease expression level. Above a certain threshold of permease numbers, a cell will be in a phenotype capable of lactose metabolism, and below this threshold, a cell will be in a phenotype incapable of lactose metabolism (*10*, *11*). The former has high fluorescence from the cell membrane, whereas the latter has low fluorescence, when the permease is labeled with a yellow fluorescent protein (YFP). The image in Figure 1B shows the coexistence of both phenotypes in a cell population at intermediate inducer concentrations, characterized by the bimodal distributions of fluorescence intensity in Figure 1C.

While it is known that the bistability in the *lac* operon arises from positive feedback (*12*, *13*), the molecular mechanism underlying the initiation of switching between two phenotypes remains unclear. Novick and Weiner deduced that switching from the uninduced state to the induced state occurs through a single rate-limiting molecular process (*12*) rather than a multi-step process. They further hypothesized that the random

expression of one molecule of permease was enough to trigger induction. However, this has never been observed experimentally because of insufficient sensitivity.

Our group has shown previously that a single fluorescent protein molecule can be visualized in a living bacterial cell using the method of detection by localization (*14-16*). Because a permease molecule is a membrane protein with slow diffusion, its fluorescence label is highly localized compared to a fluorescent protein in the cytoplasm, allowing detection above the background of cellular autofluorescence. Thus, we generated strain SX700, which possesses intact *lac* promoter elements and expresses a functional LacY-YFP fusion protein (Fig. S1) from *lacY*'s native chromosomal position (Fig. S2). Figure 1B shows a fluorescence image of SX700 cells that allows us to directly count the number of single LacY-YFP molecules present in a cell.

Figure 1D shows the histogram of permease copy numbers in the uninduced fraction of cells, free from the complication of autofluorescence background in the lower peak of Figure 1C. Evidently, the uninduced cells have zero to ten LacY molecules with significant probability, independent of the inducer concentration. Had one permease been enough to trigger induction, we would have seen that all cells in the uninduced subpopulation would possess zero LacY molecules. Thus, we conclude that a single copy of LacY is not sufficient to induce switching of the phenotype, and the threshold for induction must be much higher than several molecules per cell.

We then set out to determine the threshold of permease molecules for induction. It is experimentally difficult to capture the rare events of phenotype switching in real time. To overcome this difficulty, we prepared cells covering a broad range of permease copy numbers by first fully inducing the cells and subsequently washing out the inducer. We then allow the cells to divide for one to six generations, during which the initial permeases are partitioned into daughter cells (*17*). Figure 2A shows fluorescence time traces of the cells, normalized by cell size, upon the reintroduction of 40 μM TMG. Interestingly, while the fluorescence in cells with low permease numbers continues to decay because of cell division and photobleaching, cells with over 300 initial permease molecules induce again within three hours and show increased fluorescence. Figure 2B shows that the probability of induction as a function of initial permease number, which is well fit by a Hill equation with a Hill coefficient of 4.5 and a threshold of ~375 molecules. The large value of the threshold indicates that hundreds of permease molecules are necessary to switch the phenotype.

If the induction is due to a single rate-limiting event as Novick and Weiner argued, there must be a single large burst of permease expression to reach this high threshold. However, only small bursts have been observed in previous studies of the repressed *lac* promoter (*14, 18*). Large bursts, if any, would be infrequent and insufficiently sampled in the previous works. To explain why both small and large bursts may occur from the *lac* promoter, we consider the tetrameric repressor that is doubly bound to two operators, forming a DNA loop (*19, 20*). We hypothesize that more frequent partial dissociations of

the tetrameric repressor from one operator lead to single transcripts and small bursts of protein expression, while rare complete dissociations from all operators lead to multiple transcripts and large bursts of expression. In this model, the complete dissociation of the tetrameric repressor would be the molecular event causing a change in phenotype.

To test this model experimentally, we first removed the auxiliary operators from SX700 to generate SX702 (Fig. S2), which cannot form DNA loops. As a result, every dissociation event of LacI from the remaining O1 operator results in a complete dissociation event that would generate a large burst of expression. In this case, we predict frequent and large bursts of expression with a faster rate of phenotype switching. Indeed, Figure 2C shows that without DNA looping, SX702 induces rapidly upon addition of inducer, even though the initial permease numbers are much smaller than the threshold in Figures 2A and 2B (see Supporting Text). Interestingly, the removal of DNA looping eliminates bistability. This is manifested by the unimodal distributions of an inducing population in Figure 2D at 20 μM TMG concentrations.

To observe large bursts directly, we replaced the *lacY* gene of the *E. coli* chromosome with a membrane localized protein Tsr fused to YFP, generating strain SX701 (Fig. S2). Eliminating LacY's positive feedback serves two purposes: allowing the resolution of distinct large bursts and proving that large bursts do not require permease activity. The Tsr-YFP fusion functions as a surrogate reporter for protein production with single-molecule sensitivity.

When we acquire time-lapse fluorescence microscopy movies of SX701 cells with 200uM TMG, we observed that Tsr-YFP is produced mostly in small bursts, but occasionally in a large burst (Figures 3A). The distribution of burst sizes (Figure 3B) taken from these real-time traces, shows both the frequent, exponentially distributed small bursts and the rare, unusually large bursts.

We now analyze the inducer concentration dependence of burst frequency and size using population distributions. Figure 3C shows that SX701 has a protein copy number distribution in a cell population very similar to the distributions of uninduced cells in Figure 1D within the range of zero to ten molecules. We have shown that these copy-number distributions manifest the stochasticity in gene expression characterized by two parameters, transcription rate, *a*, and the burst size of proteins per mRNA, *b*, and can be well-fit with a gamma distribution, $p(n) = b^{-a}n^{a-1}e^{-n/b}/\Gamma(a)$ (*18, 21*). The inset in Figure 3C shows *a* and *b* determined in this fashion for cells with less than ten molecules for different TMG concentrations. The small burst size is independent of inducer concentration, whereas the small burst frequency has only a weak concentration dependence. In fact, within the range of 0 to 50 μM TMG, the small burst frequency does not change appreciably, suggesting that the partial repressor dissociation is predominantly spontaneous at low inducer concentrations.

Because characterization of the rare, large bursts is difficult for the wildtype operators,

we generated strain SX703, in which the permease gene is replaced with Tsr-YFP and the O2 and O3 operators are removed to eliminate DNA looping. Every dissociation event in the SX703 should be a complete dissociation, and hence, lead to a large burst. As there is a 20-100 fold difference in the inducer binding affinity to the repressor in DNA bound form (~1mM) compared to the free form (~10uM) (*22*, *23*), we expect to observe the stochastic dissociation of the repressor from the sole operator site and sequestration of the free repressor by the inducers at the concentrations we use (0-50uM), rather than inducer driven dissociation events.

Consequently, we expect the frequency of dissociation to remain constant as inducer concentration increases while the length of the dissociation time to increase. When we analyze the steady-state protein distributions at different inducer concentrations (Fig. 4C), by applying a generalized interpretation of the *a-b* model which estimates the number of proteins per expression bursts(see Supporting Text), we find that inducer concentration affects the size of large bursts, but not the frequency. This observation supports our model that the inducer sequesters the repressor after it stochastically dissociate from the operator and prolong its lifetime in the non-DNA bound state, leading to larger burst sizes (see Supporting Text).

Figure 4 summarized the model of induction in the *lac* operon. In the case of high inducer concentration (Fig. 4A), the repressor is actively pulled off both operator sites by the inducer, as described in Jacob and Monod's model (*6*). Under low or intermediate TMG

concentrations, however, the repressor can stochastically dissociate from one operator, independent of the inducer, as shown in Figure 4B. When the repressor partially dissociates from one operator, a small protein burst from a single copy of mRNA is generated (*14*), before the repressor rapidly rebinds to the vacant operator. When the repressor completely dissociates from both operators, multiple mRNAs are transcribed, leading to a large protein burst that surpasses the LacY threshold, initiate positive feedback, and maintain a switch in phenotype.

Why do complete dissociation events give rise to large bursts? Our group has recently shown that if a repressor dissociates from DNA, it takes a timescale of minutes for the operator to be rebound by a repressor again, because a repressor spends most of its time bound to and searching along nonspecific sequences on chromosomal DNA (*15*). In addition, there are only a few copies of the tetrameric repressors (*8*). Such a slow repressor rebinding time, compared to transcript initiation frequencies (*24*), would allow multiple copies of *lacY* mRNA to be made following a complete repressor dissociation event. Furthermore, in the presence of inducer, the nonspecific binding constant remains unchanged (*25*), but, the affinity of the inducer-bound repressor to the operator is significantly reduced, rendering specific rebinding unlikely. The large burst that results from slow repressor rebinding is an example of how a single-molecule fluctuation under out-of-equilibrium conditions can have significant biological consequences, which has been discussed theoretically in the context of cell signaling (*26*) and gene expression (*27*) but has not been experimentally observed previously.

Because inducers have a 20-100 fold weaker binding affinity for operator-bound repressor than free repressors (*22*, *23*), the inducer's role under low concentrations is not to force a dissociation event, but to simply sequester repressors already dissociated from their operators to aid in creating a large burst (see Supporting text and Fig. 3d). As the inducer concentration increases, the size of the large bursts increases as the duration of complete dissociation events increases, improving the probability that a large burst can cross the positive feedback threshold. Consequently, it is this higher probability of successful switch-on events that shifts the bimodal population towards the fully induced state as inducer concentration increases.

The biological significance of DNA looping has been discussed in the literature in terms of facilitating interactions between distance sequences and enhancing the local concentration (*19*, *20*). Here we show that DNA looping allows the control of gene regulation on multiple timescales through different kinds of dissociation events. The presence of DNA looping allows the use of rare complete dissociation events to control a bistable genetic switch.

We have demonstrated that a stochastic single-molecule event can cause a change in phenotype. It is not difficult to imagine that similar molecular events might determine more complicated phenotypes of other cells or organisms. The ability to observe and probe the properties of genetic switches at the molecular level is crucial for

understanding how cells make decisions.

REFERENCES

1. A. Arkin, J. Ross, H. H. McAdams, *Genetics* **149**, 1633-1648 (1998).

2. M. Ptashne. *A Genetic Switch: Phage Lambda Revisited*. (Cold Spring Harbor Laboratory Press, New York, 2004).

3. M. Kaern, T. C. Elston, W. J. Blake, J. J. Collins, *Nat. Rev. Genetics* **6**, 451-464 (2005).

4. D. Dubnau, R. Losick, *Mol. Microbiol*. **61**, 564-572 (2006).

5. E. Dekel, U. Alon. *Nature* **436**, 588-592 (2005).

6. J. Monod, F. Jacob, *J. Mol. Biol.* **3**, 318-356 (1961).

7. B. Müller-Hill. *The Lac Operon: A Short History of a Genetic Paradigm.* (Walter de Gruyter, New York, 1996).

8. W. Gilbert, B. Müller-Hill, *Proc. Natl. Acad. Sci. U.S.A.* **56**, 1891-1898 (1966).

9. G. N. Cohen, J. Monod, *Bacteriol. Rev*. **21**, 169-194 (1957).

10. J. M. G. Vilar, C. C. Guet, S. Leibler, *J. Cell Biol.* **161**, 471-476 (2003).

11. T. Mettetal, D. Muzzey, J. M. Pedraza, E. M. Ozbudak, A. van Oudenaarden, *Proc. Natl. Acad. U.S.A.* **103**, 7304-7309 (2006).

12. A. Novick, M. Weiner, *Proc. Natl. Acad. Sci. U.S.A.* **43**, 553-566 (1957).

13. E. M. Ozbudak, M. Thattai, H. N. Lim, B. I. Shraiman, A. van Oudenaarden, *Nature* **427**, 737-740 (2004).

14. J. Yu, J. Xiao, X. Ren, K. Lao, X. S. Xie, *Science* **311**, 1600-1603 (2006).

15. J. Elf, G. W. Li, X. S. Xie, *Science* **316**, 1191-1194 (2007).

16. X. S. Xie, P. J. Choi, G. W. Li, N. K. Lee, G. Lia, *Ann. Rev. Bioph.* **37**, 417-444 (2008).

17. N. Rosenfeld, J. W. Young, U. Alon, P. S. Swain, M. B. Elowitz, *Science* **307**, 1962-1965 (2005).

18. L. Cai, N. Friedman, X. S. Xie, *Nature* **440**, 358-362 (2006).

19. H. Krämer, *et al.*, *EMBO J*. **6**, 1481-1491 (1987).

20. S. Oehler, E. R. Eismann, H. Krämer, B. Müller-Hill, *EMBO J*. **9**, 973-979 (1990).

21. N. Friedman, L. Cai, X. S. Xie, *Phys. Rev. Lett*. **97**, 168302 (2006).

22. M. D. Barkley, A. D. Riggs, A. Jobe, S. Bourgeois, *Biochem.* **14**, 1700-1712 (1975).

23. M. Dunaway, *et al.*, *J. Biol. Chem.* **255**, 10115-10119 (1980).

24. D. Kennell, H. Riezman, *J. Mol. Biol.* **114**, 1-21 (1977).

25. A. Rezvin, P. H. von Hippel. *Biochem.* **16**, 4769-4776 (1977).

26. M. N. Artyomov, J. Das, M. Kardar, A. K. Chakraborty, A. K. *Proc. Natl. Acad. U.S.A.* **104**, 18958-18963 (2007).

27. J. E. M. Hornos, *et al.*, *Phys. Rev. E* **72**, 051907 (2005).

28. Materials and methods are available as supporting material on *Science* Online.

29. We would like to thank G. Church, A. Miyawaki, and B. Wanner for bacterial strains and plasmids, J. Hearn for technical assistance, and J. Elf, N. Friedman, and G. W. Li for helpful discussions. This work was supported by the NIH Director's Pioneer Award. P. J. C. acknowledges the John and Fannie Hertz Foundation.

Supporting Online Material

www.sciencemag.org

Materials and Methods

Supporting Text

Figs. S1-S7

FIGURE LEGENDS

Figure 1. The expression of lactose permease in *E. coli*. (A) The repressor LacI and permease LacY form a positive feedback loop. Expression of permease increases the intracellular concentration of the inducer, TMG, which causes dissociation of LacI from the promoter, leading to even more expression of permeases. Cells with a sufficient number of permeases will quickly reach a state of full induction, while cells with too few permeases will stay uninduced. (B) After 24 hours in M9 media containing 30 μM TMG, strain SX700 expressing a LacY-YFP fusion exhibits all-or-none fluorescence in a

fluorescence-phase contrast overlay. Fluorescence imaging with high sensitivity reveals single molecules of permease in the uninduced cells zoomed in on the red box from B. (C) After one day of continuous growth in media containing 0 to 50 μM TMG, the resulting bimodal fluorescence distributions show that a fraction of the population exists either in an uninduced or induced state, with the relative fractions depending on the TMG concentration. (D) The distributions of LacY-YFP molecules in the uninduced fraction of the bimodal population at different TMG concentrations, measured with single-molecule sensitivity, indicate that one permease molecule is not enough to induce the *lac* operon, as previously hypothesized (*12)*. Over 100 cells were analyzed at each concentration. Error bars are standard errors determined by bootstrapping.

Figure 2. Measurement of the threshold of permease molecules for induction. (A) Single cell time traces of fluorescence intensity, normalized by cell size, starting from different initial permease numbers. The initial LacY-YFP numbers are prepared through dilution by cell division of fully induced cells after removal of inducer. Upon adding 40 μM TMG at time zero, those cells with low initial permease numbers lose fluorescence with time as a result of dilution by cell division and photobleaching, while those cells with high initial permease numbers exhibit an increase in fluorescence as a result of reinduction. Permease molecule numbers are estimated from cell fluorescence (*28*). (B) The probability of induction of a cell within three hours as a function of initial permease number was determined using traces from 90 cells. The probability of induction, p, is fit with a Hill equation $p = y^{4.5} / (y^{4.5} + 375^{4.5})$ for initial permease number, y. The threshold

of permease numbers for induction is thus determined to be 375 molecules. Error bars are the inverse square root of sample size at each point. (C) To prove that complete dissociation of tetrameric repressor from two operators triggers induction, we constructed strain SX702 with auxiliary operators removed (no DNA looping). The figure shows single-cell traces of permease numbers in single cells grown in 40 μM TMG as a function of time. Unlike the looping strain SX700, the rapid induction of SX702 is no longer dependent on the initial number of permease molecules. This proves that phenotype switching is the result of a complete dissociation of the tetrameric repressor as shown in B. (D) In the absence of DNA looping, the entire population of strain SX702 rapidly induces in a coordinated manner from far below the threshold for a concentration as low as 20 μM TMG. DNA looping is necessary for bistability of the *lac* operon under these conditions.

Figure 3. Small and large bursts in the absence of positive feedback. In order to eliminate positive feedback from permease transport, we constructed strain SX701, replacing the lactose permease with the membrane protein fusion, Tsr-YFP. (A) Real-time traces of protein production in SX701 in 200 μM TMG. The FPs are photobleached immediately after detection to ensure that only newly produced proteins are measured after each 4 minute interval. Representative traces of single cells show frequent small bursts, associated with partial dissociation events, and a rare large burst, associated with a complete dissociation event, of protein production. (B) Distribution of burst sizes determined for 208 bursts from the real-time experiment depicted in B. Although the

majority of bursts are small, a number of unusually large bursts are observed. The former are attributed to partial dissociations, and the latter to complete dissociations of the tetrameric repressor. Inset: The occurrence of burst sizes smaller than 10 molecules is well-fit by an exponential distribution (red line). (C) Analysis of small bursts from partial dissociations of the tetrameric repressor shows that the distribution of YFP molecules in the range of zero to ten molecules does not change in the range of 0 to 200 μM TMG. A small percentage of cells have much more than ten molecules and do not appear on the axis of this plot (see Fig. S7C). Over 100 cells were analyzed for each concentration. Inset: The frequency of bursts per cell cycle, (purple circles) increases slightly while the average number of proteins per burst, (gray triangles), remains approximately constant. These kinetic parameters are determined from the steady-state distribution of YFP in those cells with less than ten molecules (see text). Error bars are standard errors determined by bootstrapping. Gamma distributions using the determined parameters are overlayed as dashed lines. The gamma distribution for 200 μM is normalized for the subpopulation of cells with less than 10 molecules. (D) In addition to having the permease replaced with Tsr-YFP, strain SX703 has the auxiliary operators removed, eliminating DNA looping so that every dissociation event is a complete dissociation. The protein number distributions should reflect the bursts of protein expression from complete dissociations alone. Inset: the noise parameters μ^2/σ^2 (purple circles) and σ^2/μ (gray triangles) suggest that the frequency of large bursts is independent of the TMG concentration but that the burst size is not.

Figure 4. Complete dissociation of the tetrameric repressor triggers induction.

(A) A high concentration of intracellular inducer can force dissociation of the repressor from its operators, as described by Jacob and Monod (*6*). (B) At low or intermediate concentrations of intracellular inducer, partial dissociation from one operator by the tetrameric LacI repressor is followed by a fast rebinding. Consequently, no more than one transcript is generated during such a brief dissociation event. However, the tetrameric repressor can dissociate from both operators spontaneously and stochastically, then sequestered by inducer such that it cannot rebind, leading to a large burst of expression. (C) A time-lapse sequence captures a phenotype switching event. In the presence of 50 μM TMG, one daughter cell of a dividing cell switches phenotype to express many LacY-YFP molecules (yellow fluorescence overlay) while the other daughter cell does not (see Movie S1).

Figure 1

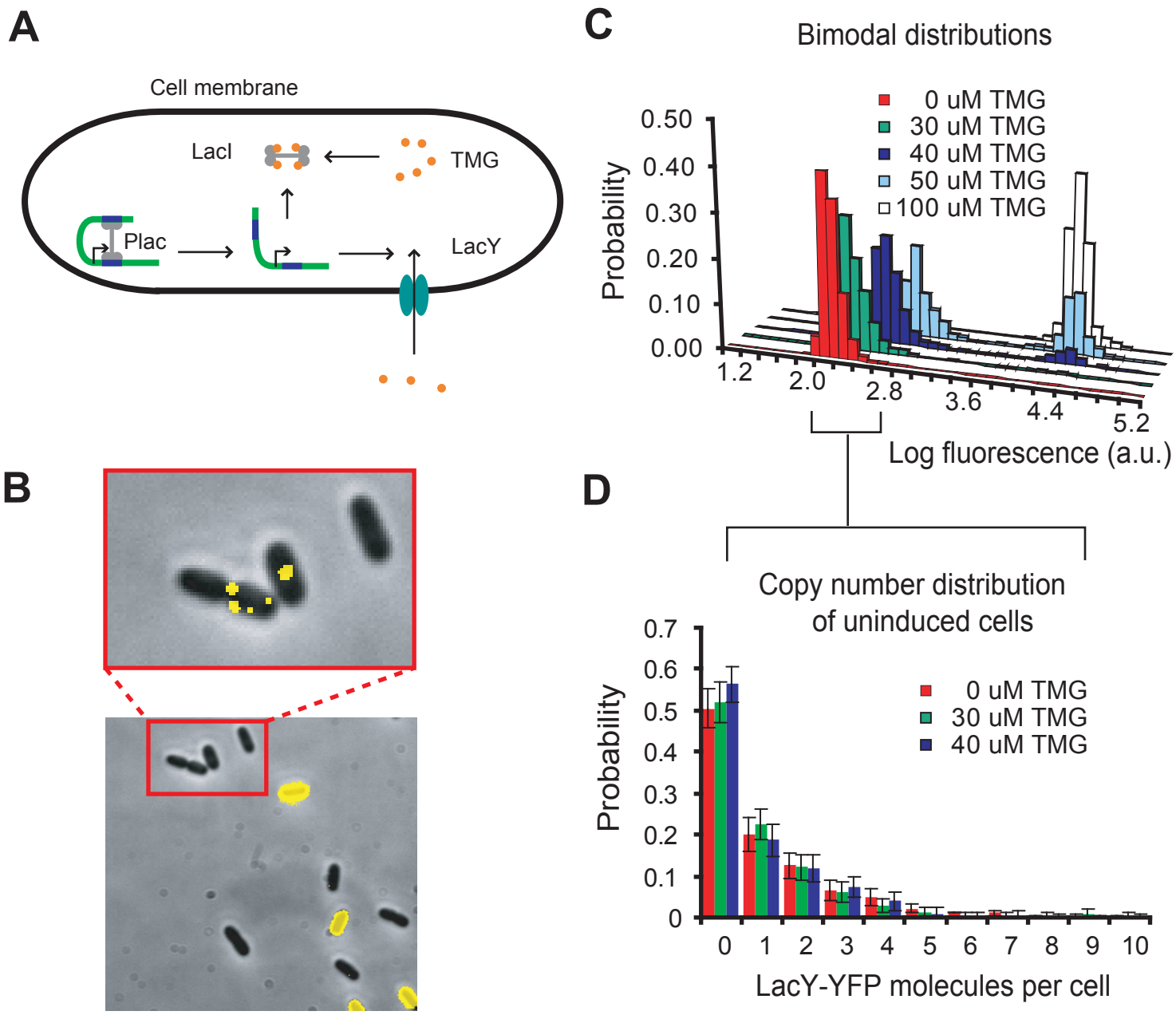
A
Cell membrane
LacI
TMG
Plac
LacY
B
C
Bimodal distributions
0 uM TMG
30 uM TMG
40 uM TMG
50 uM TMG
100 uM TMG
Probability
0.50
0.40
0.30
0.20
0.10
0.00
1.2
2.0
2.8
3.6
4.4
5.2
Log fluorescence (a.u.)
D
Copy number distribution
of uninduced cells
0 uM TMG
30 uM TMG
40 uM TMG
Probability
0.7
0.6
0.5
0.4
0.3
0.2
0.1
0
0 1 2 3 4 5 6 7 8 9 10
LacY-YFP molecules per cell

Figure 2

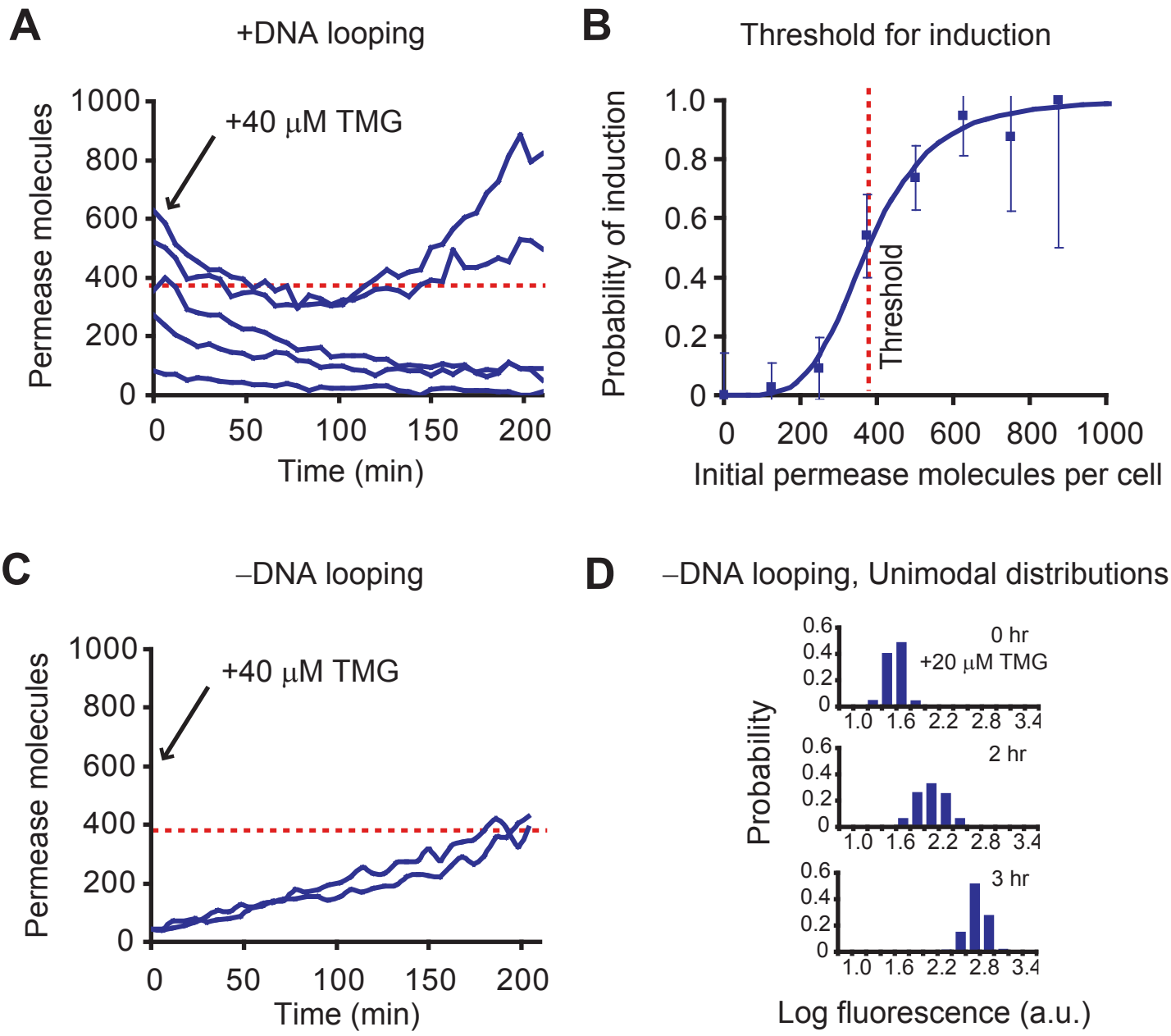
A
+DNA looping
+40 μM TMG
Permease molecules
1000
800
600
400
200
0
0
50
100
150
200
Time (min)
B
Threshold for induction
Probability of induction
1.0
0.8
0.6
0.4
0.2
0
Threshold
0
200
400
600
800
1000
Initial permease molecules per cell
C
–DNA looping
+40 μM TMG
Permease molecules
1000
800
600
400
200
0
0
50
100
150
200
Time (min)
D
–DNA looping, Unimodal distributions
Probability
0 hr
+20 μM TMG
2 hr
3 hr
0.6
0.4
0.2
0
1.0
1.6
2.2
2.8
3.4
Log fluorescence (a.u.)

Figure 3

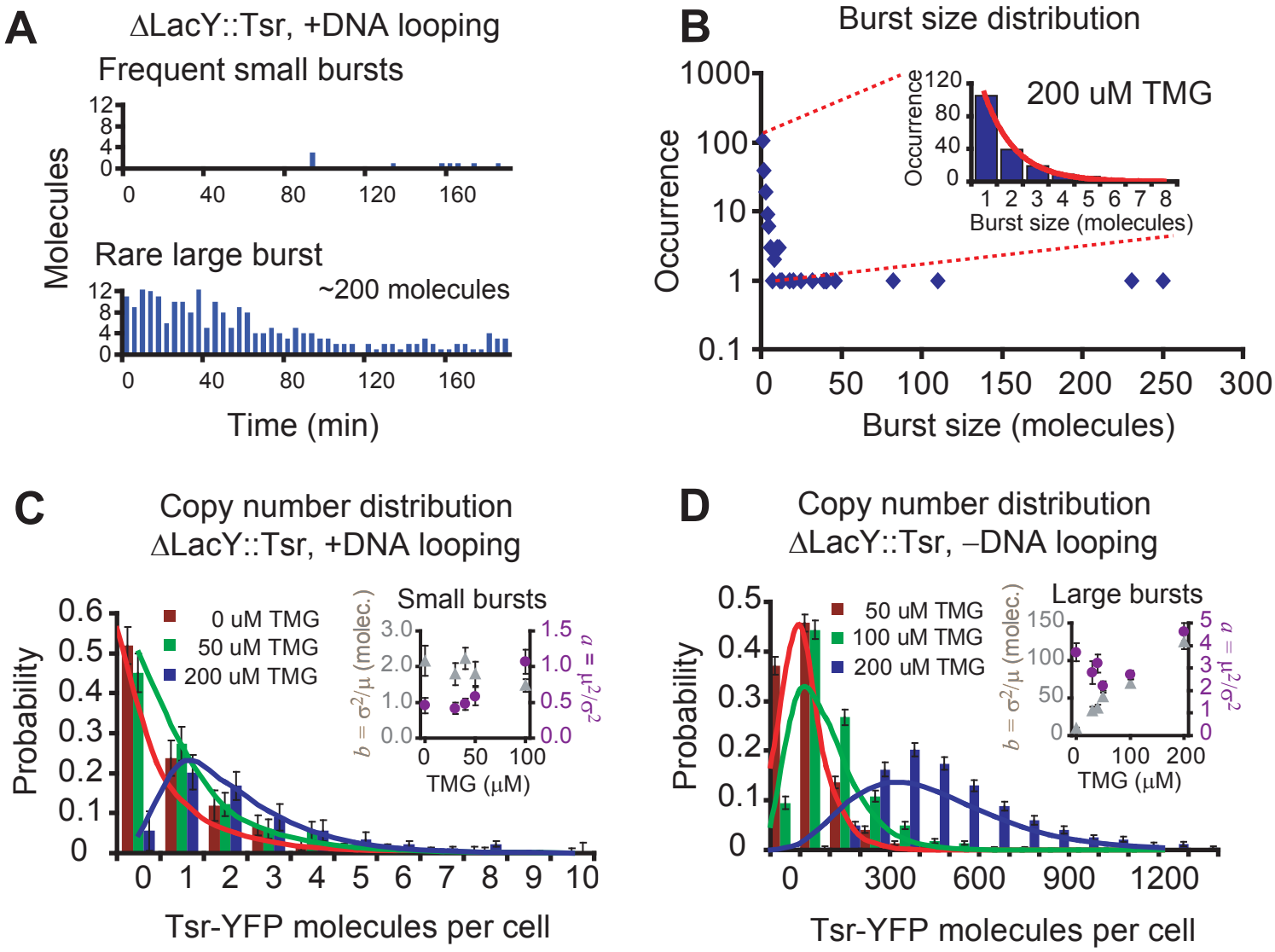
A
ΔLacY::Tsr, +DNA looping
Frequent small bursts
Molecules
Rare large burst
~200 molecules
Time (min)
B
Burst size distribution
200 uM TMG
Occurrence
Burst size (molecules)
C
Copy number distribution
ΔLacY::Tsr, +DNA looping
0 uM TMG
50 uM TMG
200 uM TMG
Probability
Small bursts
TMG (μM)
Tsr-YFP molecules per cell
D
Copy number distribution
ΔLacY::Tsr, –DNA looping
50 uM TMG
100 uM TMG
200 uM TMG
Probability
Large bursts
TMG (μM)
Tsr-YFP molecules per cell

Figure 4

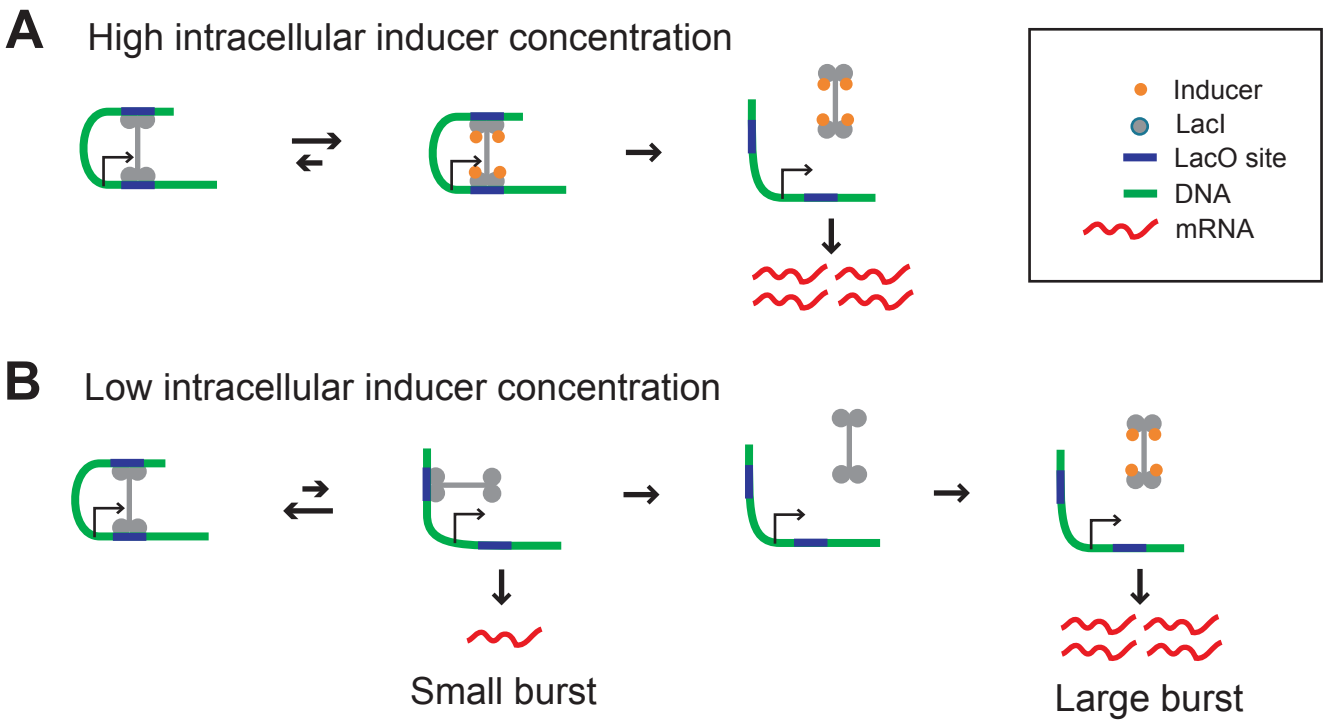
A
High intracellular inducer concentration
Inducer
LacI
LacO site
DNA
mRNA
B
Low intracellular inducer concentration
Small burst
Large burst
C
Time (min)
0
10
20
30
40
50

Supporting Online Material

MATERIAL AND METHODS

Strains and media

Strains were constructed using standard molecular biology techniques. PCR amplification was performed using on a YFP-kanamycin resistance cassette identical to the one in SX4 (*S1*) as a template. PCR was performed with primers containing overhangs targeting the desired homologous recombination by the lambda-Red system (*S2*), so subsequent electroporation into BW25993/pKD20 generated strain SX700. Similar PCR amplification of the Tsr-YFP-kanamycin cassette using strain SX4 as a template generated strain SX701. N. Friedman and J. Hearn provided plasmid pSX704, consisting of a *lac* operon region with O2 and O3 mutated to non-operator sites inserted into the pKO3 vector (*S3*). In removing the O3 operator, the CAP binding site was unperturbed in order to maintain the same effect of CAP on the promoter of all the strains. A two-step homologous recombination of pSX704 with SX700 followed by screening of the crossover site generated strain SX702. Strain and primer sequences are available on request.

Liquid cultures where shaken at 37 °C in M9 minimal media supplemented with 0.4% glycerol, amino acids, and the specified amounts of methyl- b-D-thiogalactoside (TMG).

Microscopy

Overnight liquid cultures were rediluted 100-fold in new media and grown to OD600 = ~0.1. For single-timepoint analysis, ~1 mL of the culture was pelleted by centrifugation, resuspended in ~10 uL of new media, and ~1 uL placed between two cleaned glass coverslips for imaging. For time-lapse movies, cells were pelleted and resuspended in ~50 uL of new media. Then, ~0.5 uL was placed between a 3 % agarose gel (Seaplaque) pad made with media and a glass coverslip, before assembling a imaging chamber (Bioptechs, FCS2) heated at 37 C. TMG was included in the gel pad, and a flow of fresh, prewaremd media containing TMG was also provided with a peristaltic pump at 1 mL/min. We found that continuous flow of fresh media containing inducer was necessary to provide consistent results. Images were recorded on an inverted microscope (Olympus, IX-71) with a 100x oil immersion phase contrast objective (Olympus, NA=1.35) and CCD camera (Andor, Ixon). The microscope provided an additional 1.6x internal magnification.

For single-molecule movies, a 50 ms exposure was followed immediately by 3 additional images provided photobleaching of existing fluorophores. Examination of these photobleaching images showed that the majority of fluorophores were photobleached. Excitation was provided by an Ar-Kr laser (Coherent, Innova Sabre) at 514 nm with an intensity of ~1 kW/cm^2. For induction time-lapse movies and high expression analysis,

excitation was provided by a mercury lamp (Olympus) with 300 ms exposures. Image acquisition was controlled with Metamorph software (Universal Imaging).

Data analysis

Data analysis was done though a combination of manual and automated analysis using Metamorph and custom software for Matlab (The Mathworks, Inc.). Phase contrast images were used to identify cell boundaries and the corresponding pixels from the fluorescence image used to calculate integrated cell fluorescence intensities, normalized by cell size, to construct histograms for single time-point analysis. For single molecule analysis, the number of spots provided the total number of molecules. In the case of overlapping molecules (as in the case of Tsr which oligomerizes), intensities of a 3x3 pixel square centered on the maximal peak of fluorescence intensitiy was used to determine the total number of molecules. The integrated fluorescence intensity for cells with 0 to 4 molecules, averaged over many cells, was plotted to obtain a calibration for the absolute number of YFP molecules at high levels of expression based on integration alone, as further described in the Supplemental Data. This allowed an estimate of absolute molecule numbers at high expression. For analysis of time courses for inducing cells, automatic cell segmentation was not sufficient to identify individual cells in microcolonies. Average fluorescence intensities were determined by manually highlighting cells and subtracting the background from a nearby region of pixels. For *a-b* analysis of distributions from the integrated intensity, such as in Figure 3D, a strain lacking YFP was used to subtract the mean and standard deviation due to autofluorescence. The distributions plotted in Figure 3D were obtained by deconvolution of the autofluorescence histogram with the observed fluorescence histogram using Matlab and a FFT method.

LacZ assays

β-galactosidase activity of the LacY-YFP fusion strain as compared with the parent strain in Figure S1 was analyzed using a fluorometer (Fluorolog, Jobin Yvon Spex). Cells were grown to log phase under varying concentrations of TMG. Addition of 10% chloroform by volume and vortexing for 5 seconds served to permealize them. The fluorogenic substrate, fluorescein di-β-D-galactopyranoside (FDG), was then added to a final concentration of 150 μM. β-galactosidase catalyzed hydrolysis rates were calculated from the slope of fluorescence increase.

Measurements of LacZ activity for Figure S6 were carried out using a spectrophotometer (Beckman Coulter, DU800) and a modified Miller assay with reagents and protocol from Pierce Biochemical.

Estimation of absolute permease numbers at high concentrations

The number of LacY-YFP determined by manual counting of single-molecules was

compared with the integrated fluorescence intensities for the same cells to provide a calibration of total cell fluorescence and absolute molecule numbers when using high-power, laser excitation, as shown in Figure S5, which was then extrapolated to high copy numbers. A fully induced sample was used as a control to calibrate the relative fluorescence intensities of laser and lamp excitation, allowing estimation of absolute numbers at high copies using lamp excitation.

To check the accuracy of the estimation, we note that single-molecule counting under laser excitation gives an average of one molecule in the uninduced state, and our calibration for the lamp measurement gives an average of about one thousand molecules after full induction. This thousand-fold induction agrees with our independent measurement by a Miller assay of a thousand-fold induction (*S4*). Even with an error in the estimate of absolute numbers, it is clear that the number of permease molecules necessary to force a change in phenotype is about two orders of magnitude greater than the mean number of permease molecules for uninduced cells.

SUPPLEMENTAL TEXT

Properties of LacY as a reporter and comparison with Tsr

The single-molecule measurements in strain SX700 and SX701 in media lacking inducer yielded similar values for both the mean and variance of protein expression. SX700 has an average of 0.9 molecules/cell and a standard deviation of 1.4 molecules/cell. In comparison, SX701 has an average of 1.0 molecules/cell and a standard deviation of 1.5 molecules/cell. This suggests that Tsr and LacY have similar efficiencies for translation, folding, and membrane insertion, as well as similar stability towards proteolysis. Thus, the use of Tsr as a reporter of promoter activity in the presence of inducer is justified. The similarity of Tsr and LacY results also showed that LacY dimerization was insignificant for the low copy numbers probed and did not affect the counting.

Cell membrane permeability of TMG

Our conclusions rely on the fact that TMG can diffuse into the cell even in the absence of permease molecules. Such diffusion of TMG provides a low concentration that is sufficient to sequester LacI that is dissociated from its operators (*S7, S8*). Previous measurements of TMG permeability support our conclusions. After 30 minutes of incubating permease-deficient cells with 25 μM TMG, measurement of TMG accumulation showed that the intracellular TMG concentration matched the extracellular TMG concentration (*S5*). Another measurement of TMG transport in permease-deficient cells found that the intracellular TMG reached an equilibrium level within several minutes (*S6*). From these two reports, we can conclude that the intracellular and extracellular TMG are similar and equilibrate within several minutes. Thus, in the presence of extracellular TMG in the range of 20-50 μM, we can expect a similar intracellular TMG concentration that can sequester cytoplasmic LacI and assist in

generating large bursts.

As a final note, Figure S6 clearly shows that TMG can penetrate the cell membrane and induce expression from the *lac* promoter in the absence of permease transporters.

Why one permease molecule is not enough to induce

We claim that the small number of permease molecules observed in uninduced cells (Fig. 1D) indicate that the threshold for induction must be much higher than ten molecules and argue that if one permease were enough, uninduced cells would contain zero permease molecules. The possibility that these cells are in a slow intermediate deterministically leading to induction is ruled out for two reasons. First, Figure 1C indicates that the timescale of induction is about one day. That is, a cell can spend one day in the uninduced state before transitioning into the uninduced state. The timescale of stochastic protein production and dilution from cell division in the uninduced state is about one hour. Thus, a cell will lose memory of how many molecules it has over the course of several hours because of the stochasticity of protein production. It would be impossible for a cell with one permease molecule to maintain a state of one permease molecule, or deterministically increase slowly over the course of one day, since the size of noise is larger and timescale of noise is faster.

Of course, the data in Figure 2 provides independent support of our claim regarding the threshold.

The change in repression ratio from eliminating looping is insufficient to cross the threshold

Eliminating looping in strain SX702 causes a very large change in the switching rate. Eliminating looping also causes a decrease in repression. However, the increased permease expression from the change in the repression is insufficient to cross the threshold. In the absence of permease feedback, the distribution in Figure 3D shows that the change in repression, even in the presence of 50 uM TMG, is too small for cells to cross the threshold of 375 molecules. However, Figure 2D shows that even at as low as 20 uM TMG, all cells show rapid, uniform induction.

Figure 2A further shows that even if a cell contains one or two hundred permease molecules, in the presence of looping, induction is unlikely. Such cells have even more permease molecules than would be caused by the change in repression. However, looping still prevents these cells from inducing.

Thus, a direct comparison of cells with identical numbers of permease molecules but different looping states shows that looping does indeed cause change the rate of switching by orders of magnitude, and the resulting increased permease levels caused by the absence of looping is insufficient to activate positive feedback.

Bursting properties of the *lac* promoter

The burst-like nature of gene expression in *E. coli* has been reported in three different scenarios: the fully repressed *lac* operon (*S1*, *S9*), the fully induced *lac* promoter (*S10*), and during the induction of the *lac* operon (this report). These three bursting processes result from distinct, but related, mechanisms as we describe below.

The burst-like production of proteins observed from the repressed *lac* operon in previous reports resulted from the translation of multiple proteins from a single transcript (*S1, S9*). These experiments were carried out for uninduced cells in the absence of inducer. Previously, the result was interpreted as the dissociation and rapid rebinding of the lactose repressor from its operators, allowing enough time for a single transcription event. We extend the previous interpretation by arguing that each dissociation event leading to the observed transcription is in fact only a partial dissociation event, and not a complete dissociation event.

We expect that a complete dissociation event would lead to multiple rounds of transcription, generating a different kind of large bursting. Why were large bursts resulting from complete dissociations not observed in the previous reports? Complete dissociation events occur with a frequency that is orders of magnitude smaller than partial dissociation events. The frequency of partial dissociation events leading to transcription was about once per cell cycle. The probability of observing a complete dissociation event would be too small to appear in the results. Furthermore, these experiments were carried out in the absence of inducer, which we argue is necessary for creating very large bursts through sequestration of the lactose repressor once it dissociates from its operators.

Another observation of bursting at the transcriptional level was reported for a fully induced *lac* promoter (*S10*). In the previous report, the function of the repressor is irrelevant, because the system is saturated with a high concentration of inducer. The mechanism behind the transcription bursting in the absence of repressor function is unknown. In the present report, though, we discuss a different kind of large bursting behavior that is repressor-dependent. Large bursts of multiple transcripts occur because of the rare, complete dissociation of the lactose repressor and slow rebinding time in the presence of moderate amounts of inducer.

Application of *a*-*b* bursting model to low and high protein expression

The interpretation of $a = \mu^2/\sigma^2$ and $b = \sigma^2/\mu$ as the number of transcripts per cell cycle and proteins per mRNA, respectively, was presented and validated for protein distributions from the repressed *lac* promoter (*S9*). Under repressed conditions, the partial dissociation of the tetrameric repressor leads to single transcripts, as proved in Reference S1, validating the interpretation of *a* and *b* as translational bursts for single mRNA.

However, as noted in Reference S11 and also discussed in Reference S12, the interpretation of *a* and *b* can be generalized to the case of multiple transcripts per bursting event. This interpretation is valid if the period of transcriptional activity results in a total number of proteins that are exponentially distributed per burst, even if the proteins result from multiple transcripts. Then, *a* corresponds to the frequency of these multi-transcript events, and *b* to the aggregate number of proteins per event. This scenario could likely exist, for example, for a repressor that dissociates and remains dissociated for an exponentially-disributed amount of time, during which a proportional number of mRNA are generated.

In this example, *a* corresponds to the frequency of repressor dissociation, while *b* corresponds to the total number of proteins per "large burst". Because the gamma distribution behaves as the convolution of *a* exponential distributions with average size *b*, the application of the model, whether *a* and *b* correspond to single transcripts or large, effective bursts, remains valid, if the bursting behavior can be approximated as the sum of events with exponentially-distributed sizes.

The interpretation of *a* and *b* as burst frequency and size parameters can be difficult at high expression levels, when extrinsic noise or other factors can dominate the protein noise, rather than the bursting process. However, we have observed that strong promoters including the fully induced *lac* operon have similar values of $a = \mu^2/\sigma^2 \approx 10$, and rarely above that. Thus, $a \approx 10$ may be a limit on protein noise imposed by extrinsic noise. However, below this, the interpretation of *a* is likely to be valid. Because we measure $a \approx$ 3-4 for the large bursts in Figure 3D, the interpretation of *a* as the burst frequency is better supported.

Direct burst size distribution in the presence of DNA looping and inducer

Figure 3B shows the burst size distribution determined for the data collected for the real-time traces in Figure 3A for over 200 bursts. The vast majority of the bursts (93%) have a size smaller than 10 molecules, which are well fit by an exponential distribution as predicted and observed previously (*S1, S9*). However, looking at the complete distribution shows a number of very large bursts that are not well-fit by the previous exponential distribution. The Z-score of the largest bursts range from 10 to over 200, using the mean and standard deviation of the exponential fit. The extremely large Z-scores support our interpretation of the large bursts arising from a separate physical mechanism, complete dissociations, from the small bursts, which are well-fit by an exponential distribution. Although obtaining a burst size distribution for these infrequent events is difficult, we do observe that the largest burst size observed is 250 molecules, which is a similar order of magnitude to the permease threshold measured in Figure 2. Such extremely large bursts are not observed in the absence of inducer (for example, in Reference S1).

Role of inducer in LacI dissociations and large bursts

Our model describes a single event – the complete repressor dissociation – as the event trigger a change in phenotype. The rate of phenotype switching has a dependence on inducer concentration, as evident from Figure 1C, so the complete dissociation events must be influenced by inducer. We consider here the possible role of inducer on complete dissociation events.

A key fact is that LacI repressors bound to their operator sites have lower binding constants for inducers like TMG than free LacI (*S7, 8*). The lower binding constant results from a combination of slower association rate and faster dissociation rate of TMG with LacI. At sufficiently high inducer concentrations of about 1mM, TMG can associate to LacI still bound to its operators and force a complete dissociation event. This situation occurs once a cell is fully induced with many permease molecules actively transporting TMG. The cells shown in Figure 2 initially have LacI bound to their operators at the initial time. Figure 2B shows that ~375 permease molecules concentrates TMG high enough to force a complete dissociation of LacI still bound to DNA.

Our conclusion, though, is that such forced dissociation events do not trigger phenotype switching, but only occur once the decision to change has already been made. We note that the binding constant of free LacI for TMG is in the range of 10-100 μM, which is precisely the range of bistability. Thus, in this range, once LacI spontaneously dissociates from all of its operators, it can be sequestered by 10-100 μM to generate a large burst of permease expression. It is still possible that a partially-dissociated repressor may interact with inducer, but it is unlikely for inducer to interact with a repressor head already bound to its operator.

While the inducer is unlikely interacting with fully-bound tetrameric repressor, once a dimer head dissociates, it could conceivably bind to inducer. Thus, inducer could increase the length of time of this partially-dissociated state, which would increase the probability of one RNA polymerase binding, such as demonstrated by the slight increase in burst frequency in Figure 3C. However, because the duration of each partial dissociation event is still much shorter than transcription initiation rates, only one RNA polymerase can bind and transcribe.

Since a partial dissociation is an obligatory intermediate step for a complete dissociation, stabilization of the partially-dissociated state would increase the rate of complete dissociation, but by no more than a similar factor of two. This is still not "pulling off" the bound repressor, but waiting for at least one dimer head to spontaneously dissociate.

We also point out that although the frequency may increase by only a factor of two, the induction rate increases a dramatic amount across the same TMG concentration range, as shown by the concentration dependence of the bimodal distributions in Figure 1C. The inducer may increase both the burst size (by sequestration) and burst frequency (by interacting with partial dissociations). However, since the small burst frequency only

increases by a factor of two, we argue that the dominant factor behind the concentration dependent transition rate is likely the burst size and sequestration.

Does every complete dissociation event lead to a phenotype transition? What does this mean for our model?

Following a complete dissociation, if enough permease molecules are generated, the resulting influx of inducer will be high enough to sequester the repressor permanently, and "pull off" the repressor if it does rebind (as in Figure 4A).

If, however, not enough permease molecules are made, the repressor will rebind to its operators, and the inducer concentration will be too low to "pull off" the repressor from its operators (otherwise there would be permanent induction). Then, the frequency of complete dissociations should not be changed by more than the factor of two previously discussed. The next large burst will occur randomly and be uncorrelated with the fact that a complete dissociation has recently occurred.

Thus, multiple complete dissociations may occur before a phenotype transition. However, each complete dissociation event will be a random, uncorrelated event, and the frequency of complete dissociations is very low (much less than the cell cycle). The effects of individual bursts will not be cumulative, as in the traditional model of protein noise crossing the threshold for positive feedback. The traditional model of protein noise invovles a many-step random walk, where the effect of new protein expression builds on the past protein production. Rather, the transition across the threshold will still be one large expression event, uncorrelated with prior expression events. This is the key point of our model, which means that a single molecule event will still control the phenotype transition, rather than protein noise resulting from the combined effect of many repressor dissociation events.

SUPPLEMENTAL FIGURES

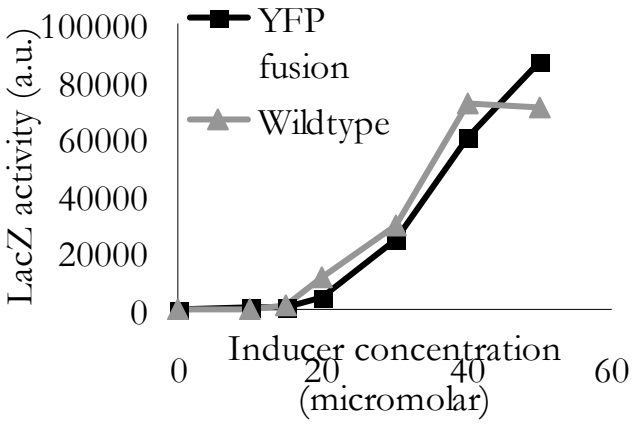

Figure S1. Permease activity of fusion protein
Induction of strain SX700 carrying a LacY-YFP fusion and the parent strain containing wildtype LacY are identical, indicating that the permease function is not perturbed by the YFP tag. Induction was measured with a fluorogenic hydrolysis assay using the substrate fluorescein-di-β-D-galactopyranoside.

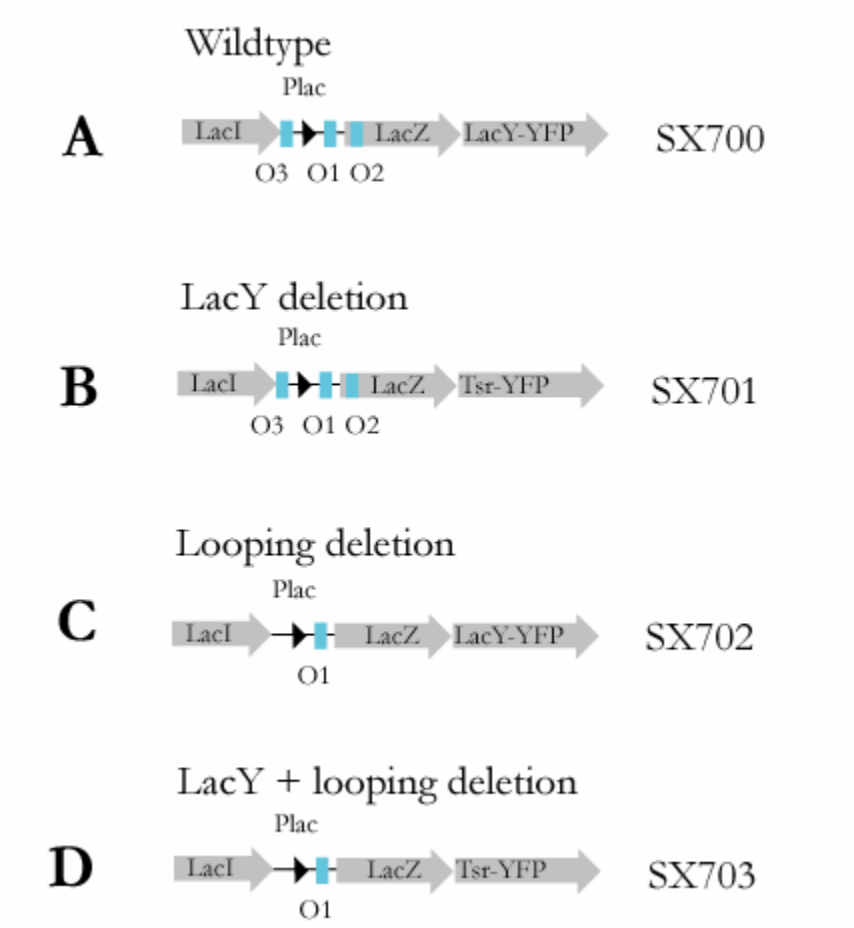

Figure S2. Srains used in this study.
(A) Strain SX700 encodes a LacY-YFP fusion with intact wildtype regulatory elements. (B) Strain SX701 replaces the lactose permease gene with the membrane protein fusion, Tsr-YFP, eliminating positive feedback from permease transport. (C) Strain SX702 lacks the auxiliary operators O2 and O3. Every dissociation of the tetrameric repressor from its single operator will result in a complete dissociation. (D) Strain SX703 contains eliminates both looping and permease function.

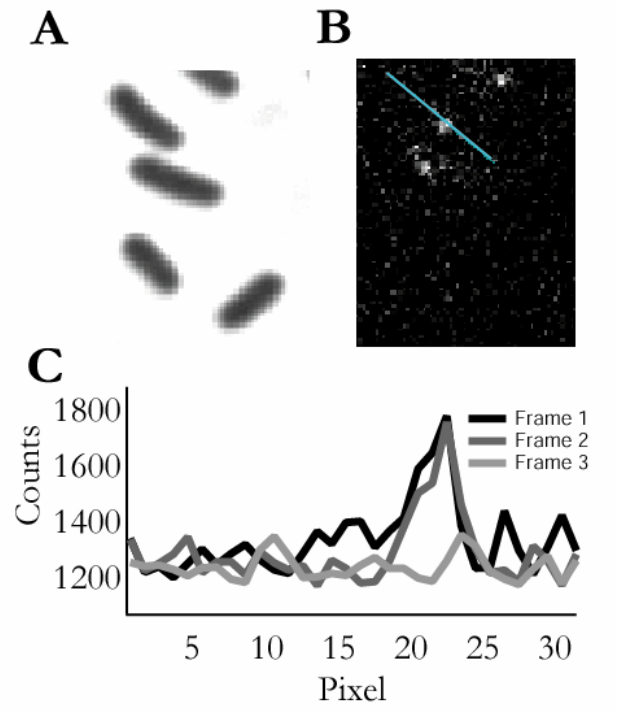

Figure S3. **Single cell detection of LacY-YFP**
A) Phase contrast image of *E. coli* cells. (B) Corresponding fluorescence image of single LacY-YFP molecules in uninduced cells. (C) Linescan of cell fluorescence for blue line in (B). Subsequent image acquisitions demonstrate single step photobleaching of the LacY-YFP molecules.

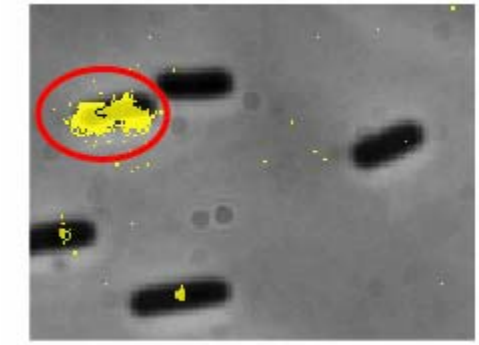

Figure S4. Strain SX701 replaces the lactose permease gene with the membrane protein fusion, Tsr-YFP, eliminating positive feedback from permease transport. After incubation in moderate amounts of TMG (50 μM TMG shown here), the majority of cells contain several YFP molecules, but cells containing much more YFP molecules are occasionally observed, as circled in red.

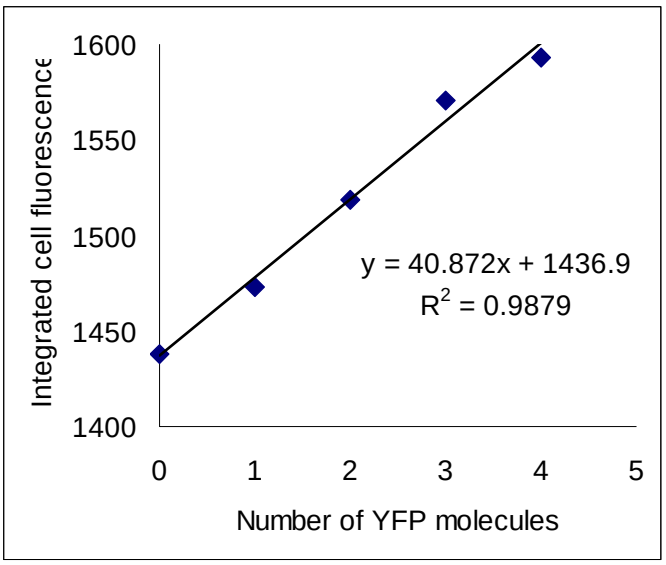

Figure S5. Absolute calibration of integrated fluorescence intensities
A linear fit of integrated fluorescence intensities (normalized by size) for cells containing 0 to 4 molecules provided a calibration for estimating YFP numbers at higher expression levels.

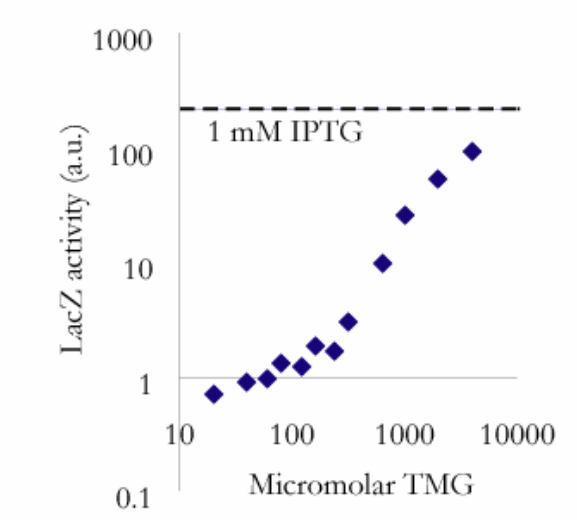

Figure S6. Induction of permease-deficient strain SX701 using ONPG assay for LacZ activity. Cells were incubated with TMG for a minimum of 12 hours before measurements. Even in the absence of specific permease transport, cells show an induction response to TMG. The average expression does not increase significantly below 500 μM TMG. In contrast, the induction rate for SX700 increases dramatically between 0 to 50 μM TMG. This suggests that the binding constant for TMG is too low to affect operator-bound repressors within the bistable concentration range, but that the TMG can interact with free repressors to assist with induction. The dual binding

constants of inducers for operator-bound and free repressor were measured in References S7 and S8.

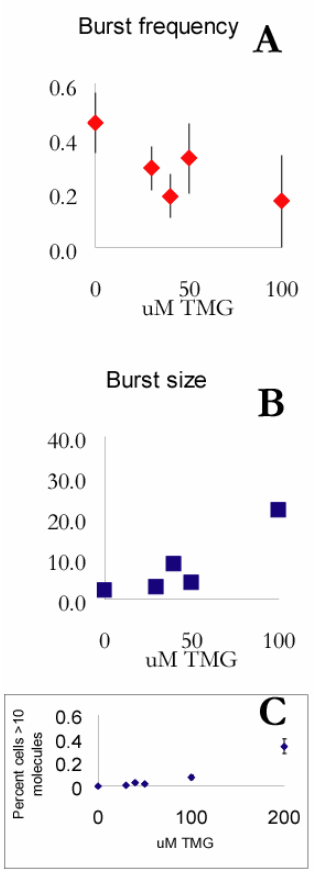

Figure S7. Burst properties of SX701.
The burst properties of permease-deficient SX701 were determined from the complete steady-state distribution (including cell with greater than ten molecules). (A) The burst frequency, calculated as the inverse of the coefficient of variation. (B) The burst size, calculated as the Fano factor. The interpretation of burst size and frequency is complicated by the presence of both small and large bursts. However, the increase in Fano factor is consistent with a greater contribution from the large bursts. (C) The percentage of cells with more than 10 molecules increases as TMG concentration increases. The rare occurrence of these high expression cells makes their quantitative characterization difficult.

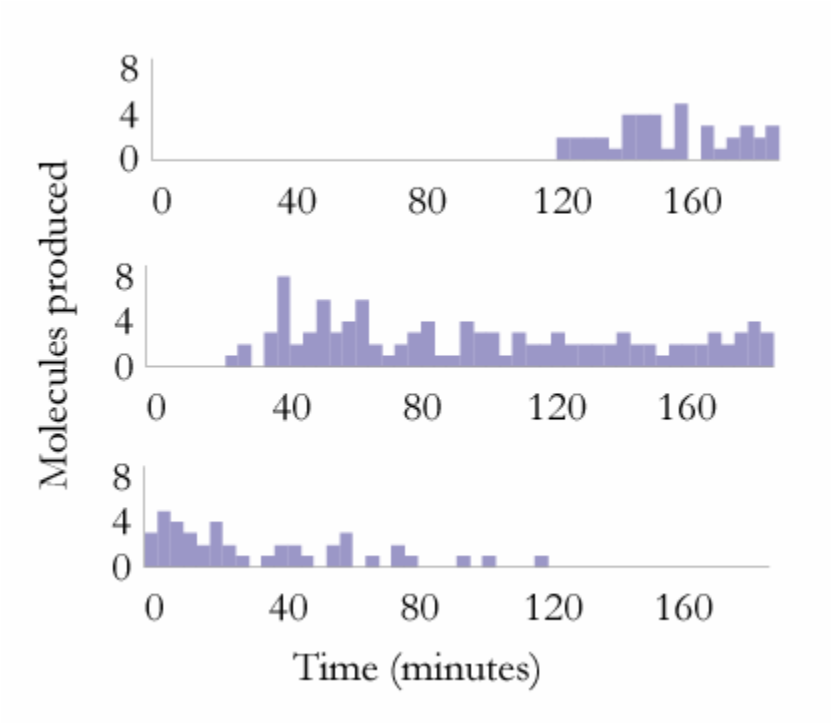

Figure S8. Large bursts events for SX701.
Three additional examples of large burst events for SX701 in the presence of 200 μM TMG are shown, similar to Figure 3A.

SUPPLEMENTAL MOVIE

Movie S1. Fluorescence overlay on phase contrast time-lapse. One daughter cell of a dividing cell switches its phenotype and expresses many LacY-YFP molecules, while the other daughter does remains in a phenotype with low expression. Cells were immobilized with polylysine in a flow cell with a continual flow of fresh M9 minimal media supplemented with amino acids and 50 μM TMG. Each frame of the movie corresponds to a 2 minute time-lapse.

SUPPLEMENTAL REFERENCES

S1. J. Yu, J. Xiao, X. Ren, K. Lao, X. S. Xie, *Science* **311**, 1600-1603 (2006).

S2. K. A. Datsenko, B. L. Wanner, *Proc. Natl. Acad. Sci. U.S.A.* **97**, 6640-6645 (2000).

S3. A. J. Link, D. Phillips, G. M. Church, *J. Bacter.* **179**, 6228-6237 (1997).

S4. S. Oehler, E. R. Eismann, H. Krämer, B. Müller-Hill, *EMBO J.* **9**, 973-979 (1990).

S5. J. L. Flagg, T. H. Wilson. *J. Bacter.* **128**, 701-707 (1976).

S6. E. A. Matzke, L. J. Stephenson, R. J. Brooker, *J. Biol. Chem.* **267**, 19095-19100 (1992).

S7. M. Dunaway, J. S. Olson, J. M. Rosenberg, O. B. Kallai, R. E. Dickerson, K. S. Matthews, *J. Biol. Chem.* **255**, 10115-10119 (1980).

S8. M. D. Barkley, A. D. Riggs, A. Jobe, S. Bourgeois, *Biochem.* **14**, 1700-1712 (1975).

S9. L. Cai, N. Friedman, X. S. Xie, *Nature* **440**, 358-362 (2006).

S10. I. Golding, J. Paulsson, S. M. Zawilski, E. C. Cox, *Cell* **123**, 1025-1036 (2005).

S11. N. Friedman, L. Cai, X. S. Xie, *Phys. Rev. Lett*. **97**, 168302 (2006).

S12. L. Cai. Thesis. Harvard University.